

Electronic Supplementary Information

Photo-responsive Anti-Fouling Polyzwitterionic Brushes: A Mesoscopic Simulation

*Zhaohong Miao, Jian Zhou**

School of Chemistry and Chemical Engineering, Guangdong Provincial Key Lab for Green
Chemical Product Technology, South China University of Technology, Guangzhou
510640, P. R. China

* Corresponding author E-mail: jianzhou@scut.edu.cn (J. Zhou.)

Content

Table S1 Repulsive parameters a_{ij} between different beads of TFC film and protein

Table S2 The dielectric constants of systems

Fig. S1 Water distribution in the simulation box of $A_{63}B_{10}C_{40}$ systems under *vis* light exposure, with $D = 0.160$ **(a)**, 0.230 **(b)** and 0.314 **(c)**, respectively.

Fig. S2 RMSD profiles of brushes from *vis* light exposure to UV exposure with $D = 0.230$, in $A_{63}B_{10}C_{40}$ system **(a)** and $A_{63}B_{10}C_{70}$ system **(b)**.

Table S1 Repulsive parameters a_{ij} between different beads of TFC film and protein (blue: the polar amino acid; orange: the moderate polar amino acid; red: the hydrophobic amino acid)

Type a_{ij}	A	Average B	Average C	Average C2	Average F	Average				
ASP	101.74	102.45	110.13	109.62	103.36	100.17	129.49	136.12	104.41	106.94
GLU	99.59		108.91		90.89		145.16		107.83	
LYS	111.97		106.62		98.05		147.68		114.01	
ARG	101.81		106.84		114.26		123.58		103.02	
SER	114.80		123.07		119.07		132.18		118.27	
THR	86.15		97.28		98.69		144.82		111.02	
PRO	100.97		110.85		98.42		124.38		106.87	
ASN	99.62		106.83		94.42		138.08		105.19	
GLN	105.42		116.01		84.41		139.74		91.83	
ALA	91.61	95.09	102.27	102.22	107.12	98.17	152.79	137.87	114.57	109.32
GLY	94.25		107.19		105.27		128.20		115.19	
CYS	77.01		87.08		96.36		134.51		110.71	
HIS	107.11		109.95		90.19		137.53		96.24	
TYR	105.48		104.62		91.90		136.34		109.91	

ILE	101.92	102.72	110.88	108.53	97.00	92.71	128.93	140.84	106.92	107.09
LEU	97.21		110.36		93.74		155.11		106.78	
VAL	110.13		113.98		102.19		146.20		98.78	
PHE	102.11		106.52		87.88		145.56		108.92	
MET	94.79		104.81		85.60		142.06		110.44	
TRP	110.19		104.62		89.86		127.19		110.70	

Table S2 (a) The dielectric constants of the systems with $D = 0.160$, $R = 0.136$, $L = 4 / 7$

ϵ_r	type	
	SP-form	MC-form
$A_{63}B_{10}C_{40}$	2.501	29.061
$A_{63}B_{10}C_{70}$	2.397	39.225

Table S2 (b) The dielectric constants of the systems with $D = 0.230$, $R = 0.068, 0.136, 0.205$, $L = 4 / 7$

ϵ_r	type	
	SP-form	MC-form
$A_{68}B_5C_{20}$	2.424	18.592
$A_{68}B_5C_{35}$	2.366	26.766

A ₆₃ B ₁₀ C ₄₀	2.349	29.013
A ₆₃ B ₁₀ C ₇₀	2.277	39.218
A ₅₈ B ₁₅ C ₆₀	2.297	36.324
A ₅₈ B ₁₅ C ₁₀₅	2.223	46.801

Table S2 (c) The dielectric constants of the systems with D = 0.314, R = 0.136, L = 4 / 7

ϵ_r	type	
	SP-form	MC-form
A ₆₃ B ₁₀ C ₄₀	2.257	28.984
A ₆₃ B ₁₀ C ₇₀	2.204	39.214

According to the work of Yang *et al.*¹, the dielectric constants were listed in Table S2. To reflect ϵ_r in P(ACN-*r*-BBEM)-*g*-SPMA and BSA systems, there was a reasonable approximation to estimate it according to molecular structure. Namely, ϵ_r is related to the number of hydrophobic and hydrophilic beads in the coarse-grained model. The hydrophobic beads are mainly composed of alkanes with ϵ_r about 2.0. The hydrophilic beads are soluble in water surrounded by water beads, therefore, ϵ_r can be set as 78.0 (dielectric constant of water at the room temperature). Thus, the system ϵ_r can be expressed as:

$$\epsilon_r = \frac{n_{\text{hydrophilic}} * 78.0 + n_{\text{hydrophobic}} * 2}{n_{\text{hydrophilic}} + n_{\text{hydrophobic}}}$$

where $n_{\text{hydrophilic}}$ means the total number of hydrophilic beads of polymers in the system, and $n_{\text{hydrophobic}}$ means the total number of hydrophobic beads of polymers in the system.

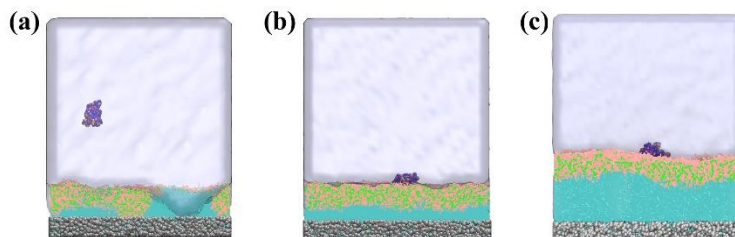


Fig. S1 Water distribution in the simulation box of $A_{63}B_{10}C_{40}$ systems under *vis* light exposure, with $D = 0.160$ (a), 0.230 (b), 0.314 (c), respectively.

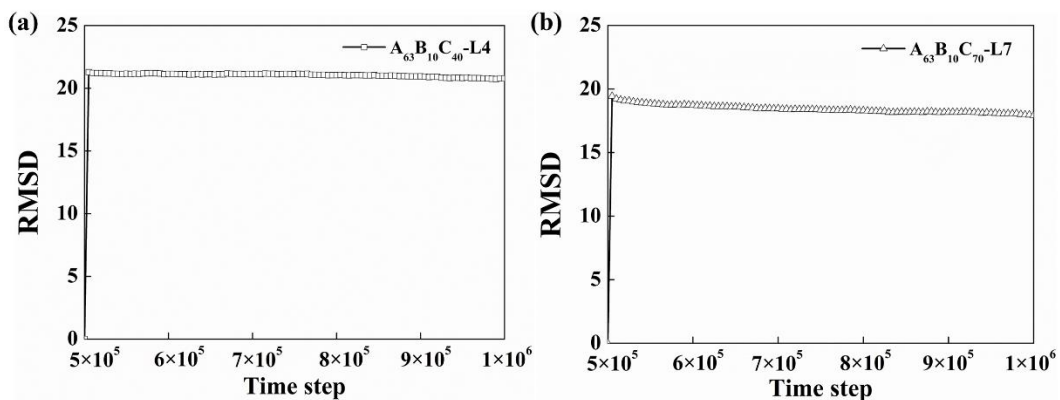


Fig. S2 RMSD profiles of brushes from *vis* light exposure to UV exposure with $D = 0.230$, in $A_{63}B_{10}C_{40}$ system (a) and $A_{63}B_{10}C_{70}$ system (b).

In Fig. S2, RMSD data of brushes from the SP form to the MC form in system of $A_{63}B_{10}C_{40}$ are shown. As light switches from *vis* to UV, in the first 1×10^5 steps, the RMSD curve rises sharply, namely, the conformation of brushes changes obviously. Under *vis* exposure, the chain with SP form is in a shrank state and the size is smaller; when

experiencing UV radiation, the chain swells apparently and the size increases obviously. Those results confirm the reasonability of the R_g^2 data of system $A_{63}B_{10}C_{40}$, as well as explain the thickening of the selective layer. Namely, the swelling hydrophilic selective layer can supply a strong mechanical push to remove the foulant. Fig. S2b displays the RMSD data of $A_{63}B_{10}C_{70}$ system. Although the RMSD curve also rises sharply in the first 1×10^5 steps, the equilibrium value is slightly less than that of $A_{63}B_{10}C_{40}$ system. That is, the conformation stability of chain in $A_{63}B_{10}C_{70}$ system is higher than that of $A_{63}B_{10}C_{40}$ system. The longer brush-hair causes a stronger steric-hindrance effect to limit the deformation of brushes and creates a tighter hydration layer when experiencing UV radiation. Therefore, the R_g^2 values in $A_{63}B_{10}C_{70}$ system shows opposite change trend compared with those in $A_{63}B_{10}C_{40}$ system. While the antifouling ability of the system become enhanced.

REFERENCE

1. Yang, S. C.; Zhu, Y. L.; Qian, H. L.; Lü, Z. Y. Molecular dynamics simulation of antipolyelectrolyte effect and solubility of polyelectrolytes. *Chem Res Chinese U* **2017**, 33 (2), 261-267 DOI: 10.1007/s40242-017-6354-0.